

Supporting Information

Ultrathin Fe-MOF modified by Fe₉S₁₀ for highly efficient oxygen evolution reaction

Wenjing Shang, Binghao Wang, Xin Deng, Yiqin Tian, Yongbing Lou, Jinxi Chen *

School of Chemistry and Chemical Engineering, Jiangsu Engineering Laboratory of Smart Carbon-Rich Materials and Device, Southeast University, Nanjing 211189, PR China

**Corresponding author*

**E-mail address: chenjinxi@seu.edu.cn (J. Chen)*

1. Calculation formulas

The calculation formulas used in this paper were showed as follows:

Overpotential: $\eta = E_{\text{RHE}} - 1.23 \text{ V}$, $E_{\text{RHE}} = E_{\text{Ag/AgCl}} + 0.059 * \text{pH} + 0.197 \text{ V}$

where E_{RHE} referred to reversible hydrogen electrode potential.

Tafel slope: $\eta = b \log j + a$,

where b was the Tafel slope. It was derived from the LSV curve, $\log j$ (j was the current density) as the abscissa and η as the ordinate, and the resulting slope was called the Tafel slope.

$2C_{\text{dl}}$ is estimated by plotting $\Delta J = (J_{\text{a}} - J_{\text{c}})$ at 0.94 V against the scan rates.

Faradic efficiency: $\text{FE} = (V/V_{\text{m}})/n$,

Where V represents the actual volume of O₂ collected, V_{m} represents the molar volume of gas at the corresponding temperature at the time of the test. n represents the number of molars of gas theoretically released.

Turnover Number: $\text{TON} = n_{\text{O}_2}/n_{\text{cat}}$, where n_{O_2} is the number of molars of generated O₂, n_{cat} is the number of molars of catalyst.

Turnover Frequency: $\text{TOF} = \text{TON}/t$, where t is time

2. Chemical

Urea (CH₄N₂O, ≥99.0%), ammonium fluoride (NH₄F, ≥98.0%), iron nitrate nonahydrate (Fe(NO₃)₃·9H₂O, ≥99.9%), sodium sulfide nonahydrate (Na₂S·9H₂O, ≥98.0%), 1,4-benzenedicarboxylic acid (C₈H₆O₄, ≥99.0%), sodium hydroxide (NaOH, ≥97.0%), and N,N-dimethylformamide (DMF, ≥99.5%) were purchased from Aladdin (Shanghai). Hydrochloric acid

(HCl, 36%~38%) and ethanol (C_2H_5OH , $\geq 99.5\%$) were bought from Sinopharm Chemical Reagent Co., Ltd (Shanghai). Ultrapure water and nickel foam (NF) were bought from Crystal chemical (Nanjing). The above chemical was used directly without further treatment.

3. The preparation of NF

Due to the presence of dirt and oxidation layers on the surface of NF, it was necessary to clean before using. The NF purchased was cut to the size of $1 \times 1.5 \text{ cm}^2$, and then it was immersed in the 3 M HCl solution prepared in advance. Cleaning with an ultrasonic cleaner for 20 minutes was employed. Then deionized water and ethanol were used for ultrasonic cleaning for 10min respectively, and then the NF was dried under vacuum at $60 \text{ }^\circ\text{C}$ for 12 h.

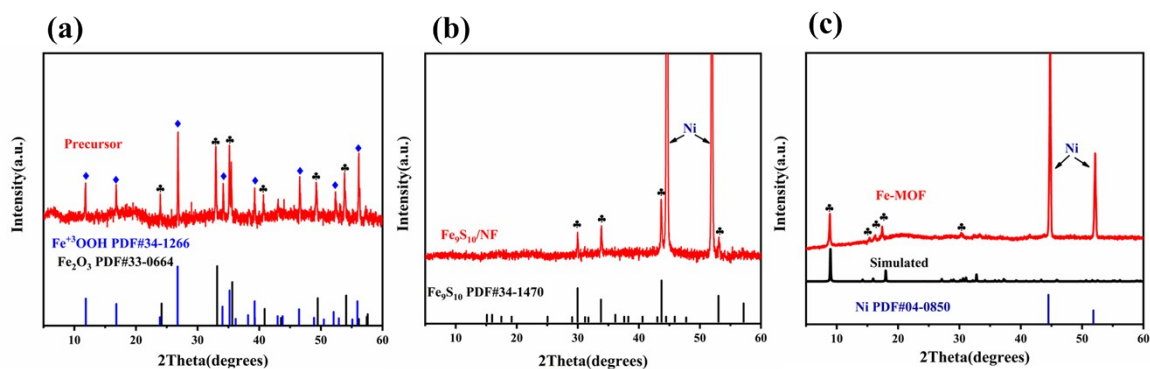


Fig. S1. XRD patterns of a) precursor, b) Fe_9S_{10}/NF and c) $Fe-MOF/NF$

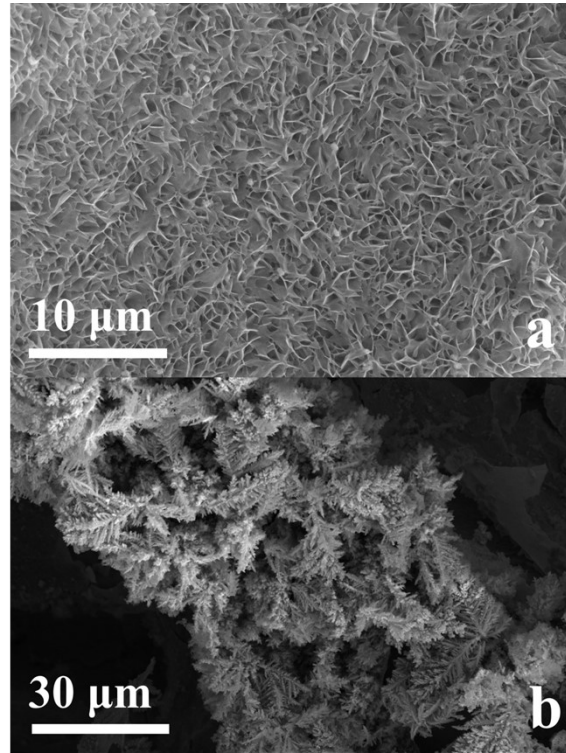


Fig. S2. SEM images of a,) Fe-MOF/NF, b) Fe_9S_{10} /NF

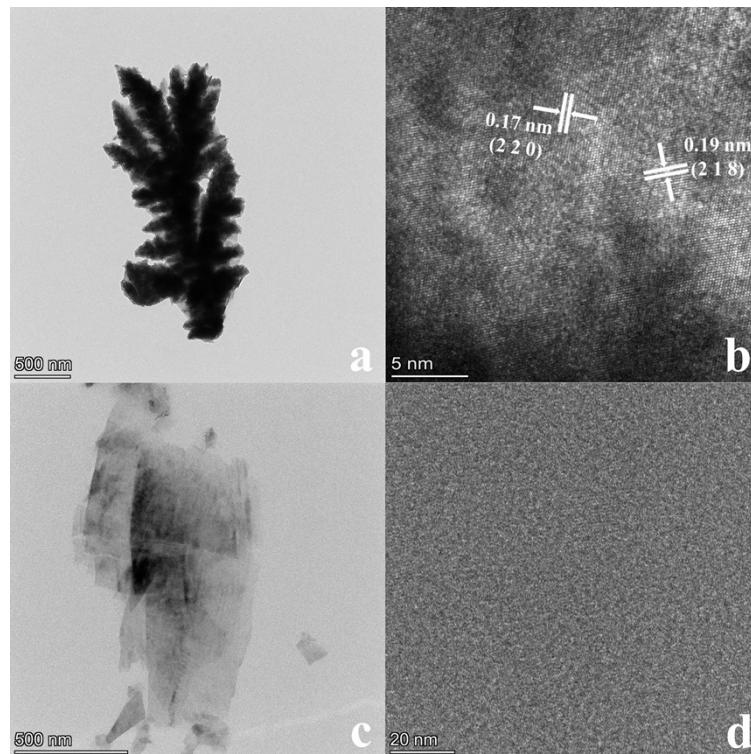


Fig. S3. TEM images of a, b) Fe_9S_{10} /NF, c, d) Fe-MOF/NF

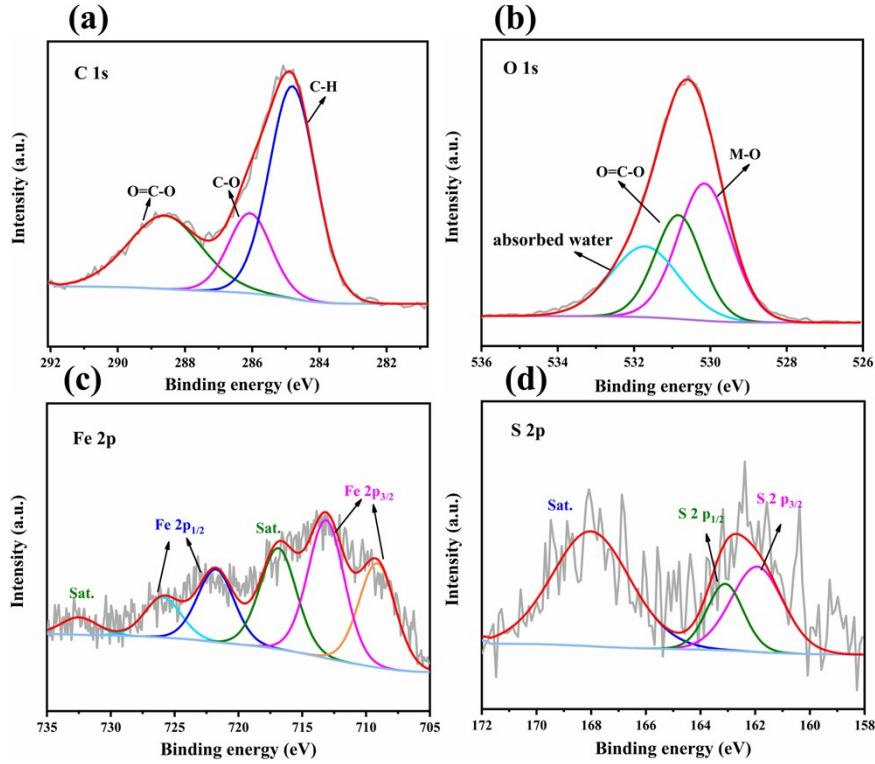


Fig. S4. XPS spectra of C1s, O1s, Fe2p, S2p in Fe₉S₁₀/Fe-MOF/NF-2 before OER

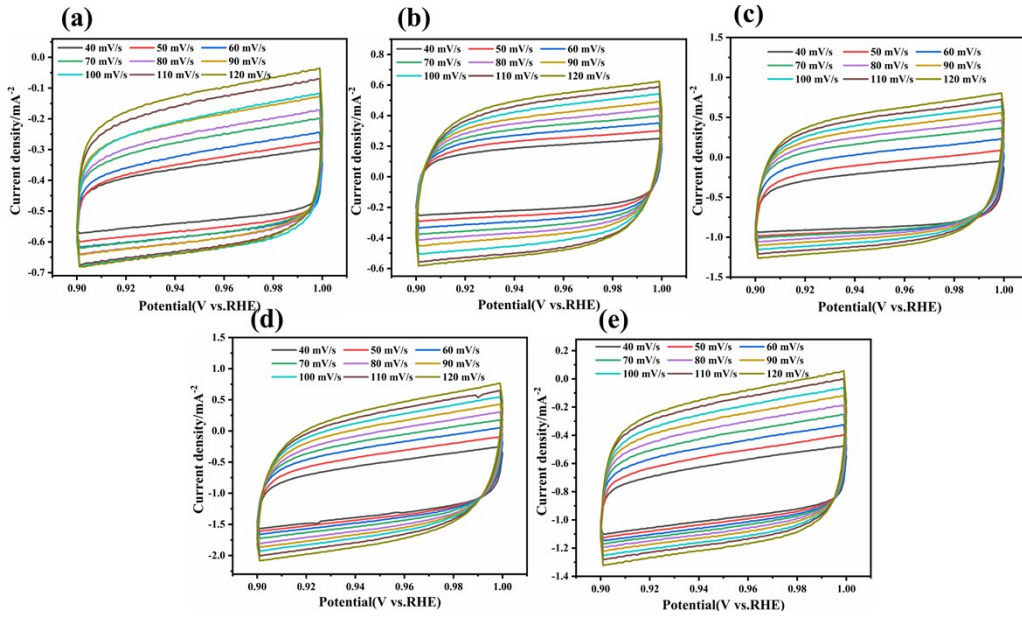


Fig. S5. CV curves of a) Fe-MOF, b) Fe₉S₁₀/NF, c) Fe₉S₁₀/Fe-MOF/NF-1, d) Fe₉S₁₀/Fe-MOF/NF-2, e) Fe₉S₁₀/Fe-MOF/NF-3 at different scan rates

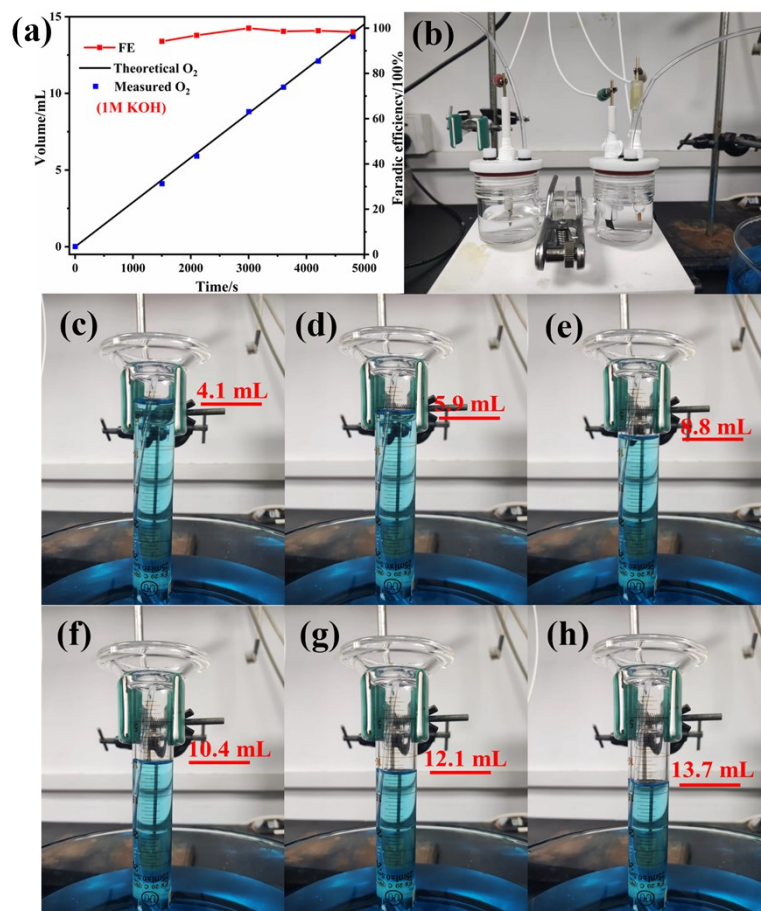


Fig. S6 a) Faradic efficiency, b) the device of drainage gas collection method, c-h) the volume of oxygen collected over time in 1 M KOH

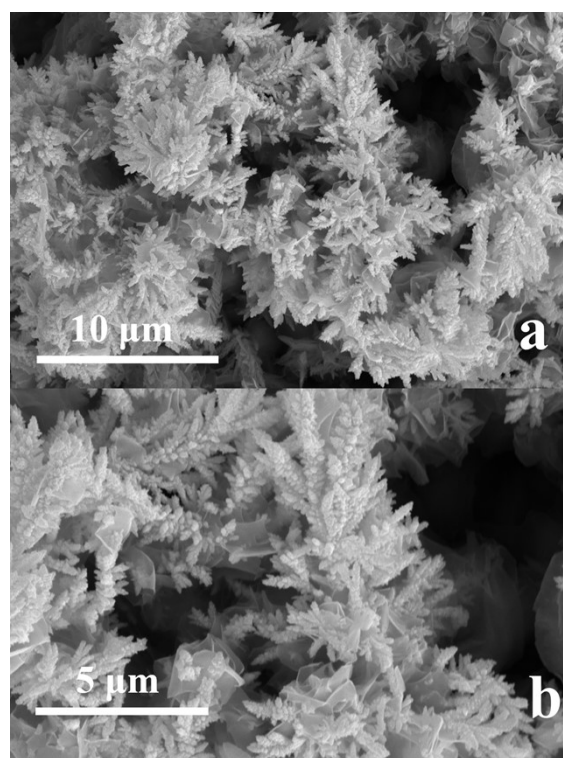


Fig. S7. SEM images of Fe₉S₁₀/Fe-MOF/NF-2 after OER

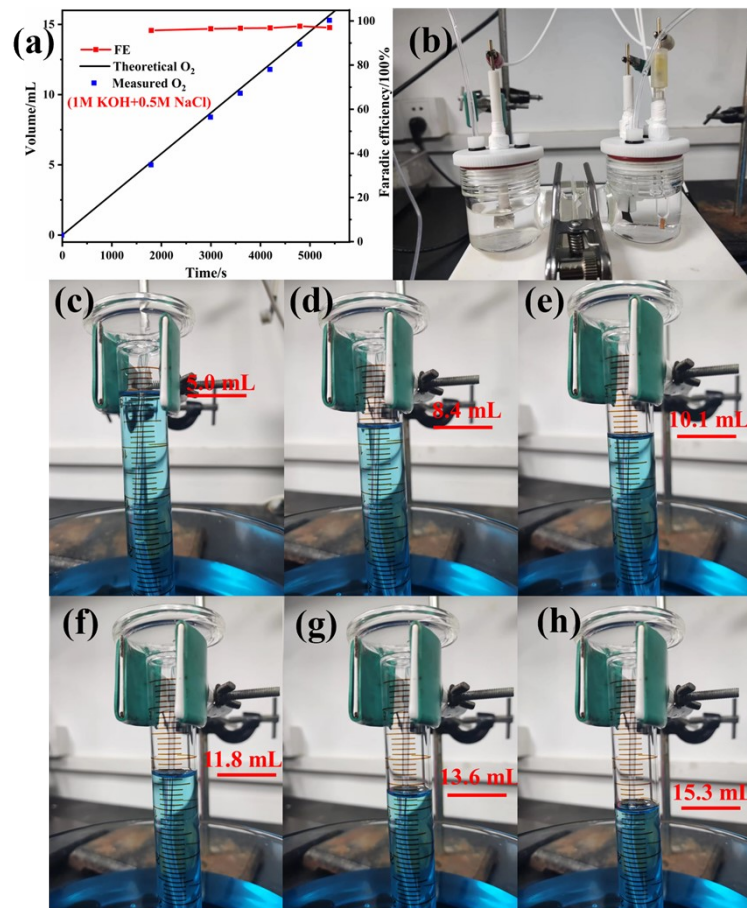


Fig S8 a) Faradic efficiency, b) the device of drainage gas collection method, c-h) the volume of oxygen collected over time in 1 M KOH+0.5M NaCl

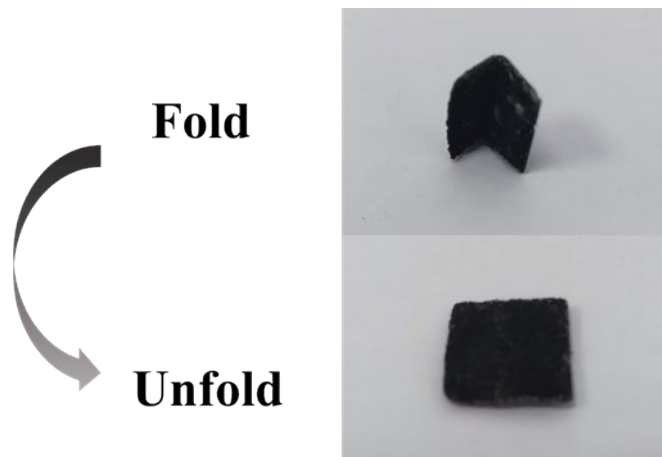


Fig. S9. Photos of Fe₉S₁₀/Fe-MOF/NF-2 when folded and unfolded

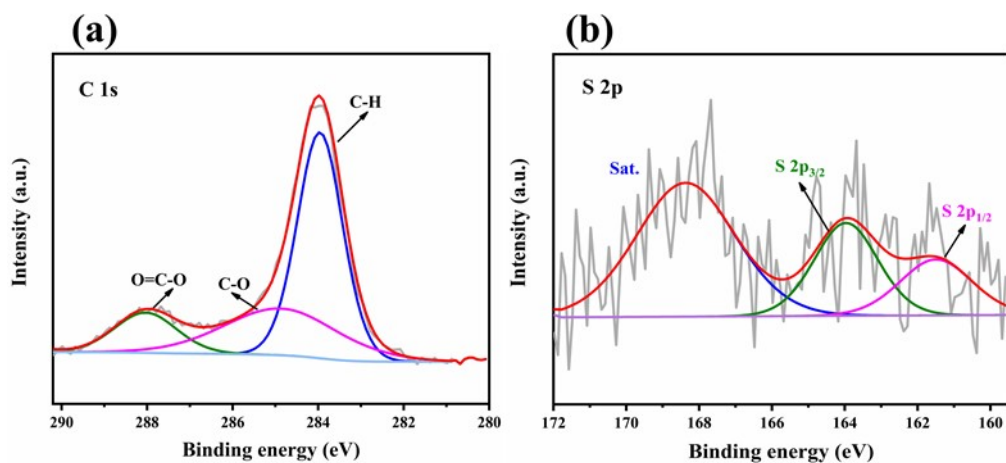


Fig. S10. XPS spectra of C1s, O1s in Fe₉S₁₀/Fe-MOF/NF-2 before OER

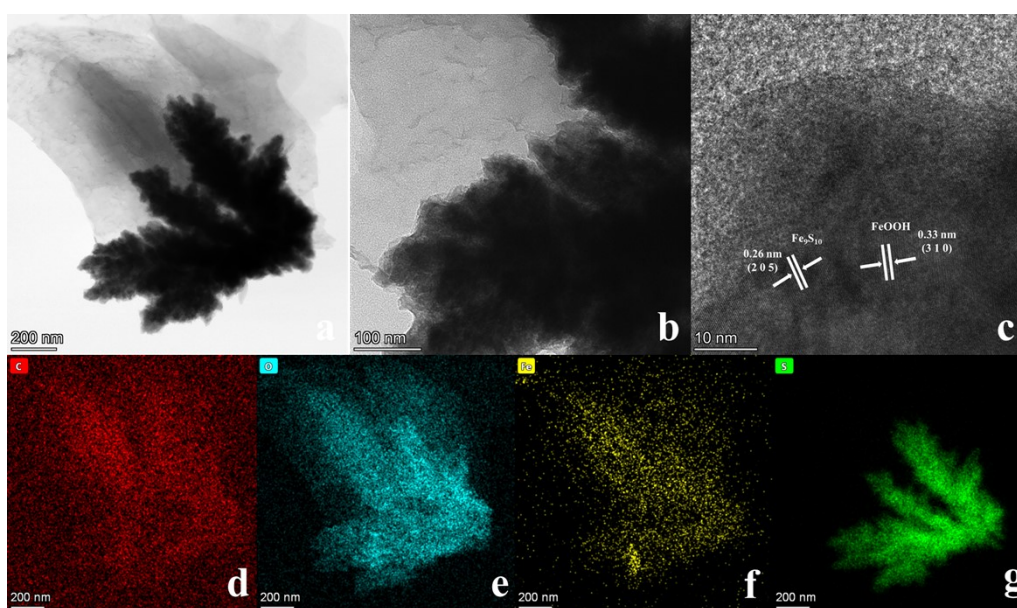


Fig. S11. a, b) TEM images, c) HRTEM images, d, e, f, g) elemental mapping of Fe₉S₁₀/Fe-MOF/NF after OER

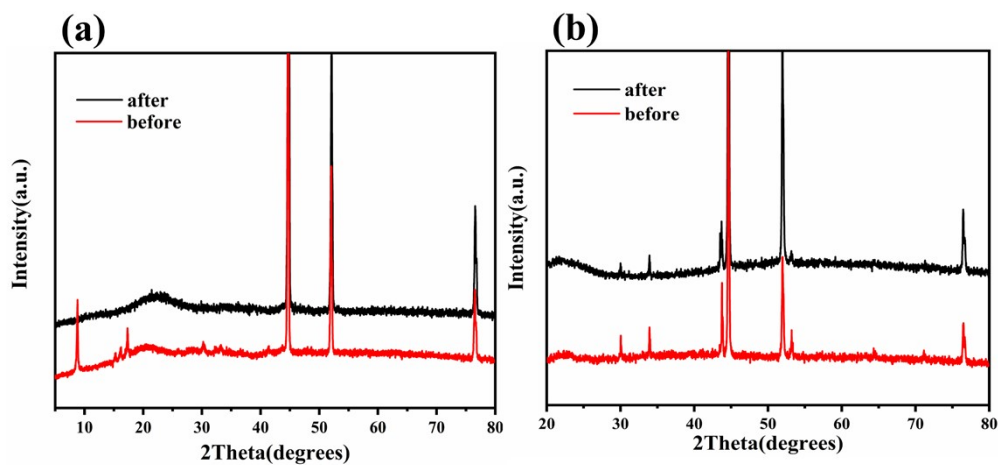


Fig. S12. XRD patterns of a) Fe-MOF/NF, b) Fe₉S₁₀/NF before and after reaction

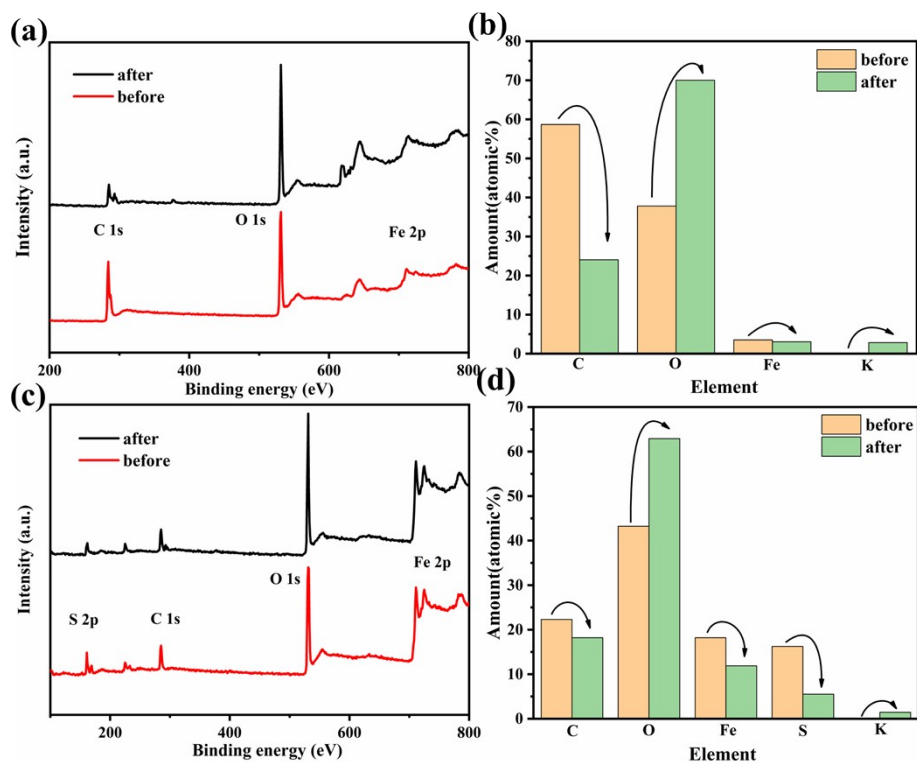


Fig. S13. survey spectrum of a) Fe-MOF/NF, c) Fe₉S₁₀/NF, and the changes in the content of elements of b) Fe-MOF/NF, d) Fe₉S₁₀/NF before and after OER test

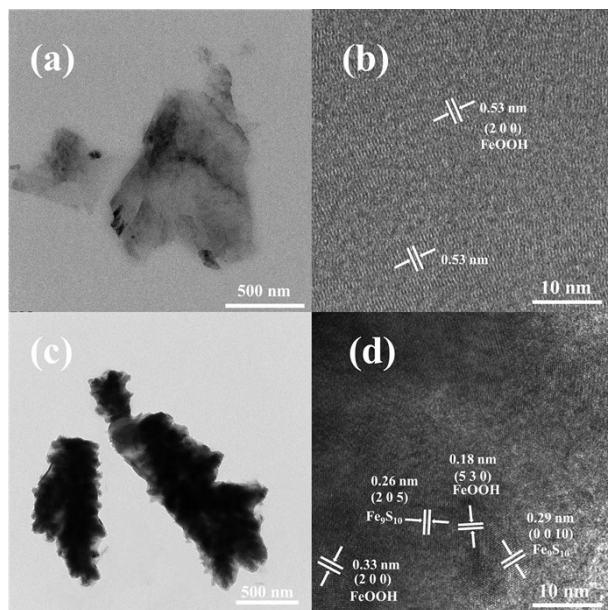


Fig. S14. TEM images of a) Fe-MOF/NF, c) Fe₉S₁₀/NF and HRTEM images of b) Fe-MOF/NF, d) Fe₉S₁₀/NF after reaction

Table S1. Comparison of OER performance in this work with recently reported materials introduced into S by the postprocessing of precursors electrocatalysts

Catalysts	Overpotential (mV)/ current density (mA cm ⁻²)	Tafel slope (mV/dec)	Stability time (h)	Support	Reference

Fe₉S₁₀/Fe-MOF/NF-2	202/10, 225/50	34	90	NF	This work
Ni ₃ S ₂ /MIL-53(Fe)	214	33.8	23	NF	1
CoMoO ₄ /Fe-MOF	238	49	30	NF	2
NiMoO ₄ /Ni-MOF/NF	218	68	20	NF	3
Co ₃ O ₄ @Co-MOF	277	79	-	GC	4
NM50-Ni ₃ S ₄ /NF	257	67	300	NF	5
S-NiFe(CN) ₅ NO-500	274	54	30	GC	6
Fe _{0.5} Ni _{0.5} Co ₂ -S/NF	251/50	73	25	NF	7
NiCo ₂ S ₄ /CC	290/50	139	10	CC	8
CoS ₂ -MoS ₂ HNAs/Ti	266	104	24	TF	9
Cr-NiS ₂ /C@NF	207	43	80	NF	10
PBA-SA	261	38	15	RD	11
FeNi ₂ -400-S	214	80	12	GC	12
Co ₉ S ₈ /Zn _{0.8} Co _{0.2} S@C	292	52	5.5	GC	13
NiCo ₂ S ₄ /FeOOH	200	71	20	CC	14

NF: Ni Foam

CC: Carbon Cloth

GC: Glassy Carbon

TF: Ti Foil

RD: Rotating Disk

Table S2 The TON and TOF of catalysts

Catalysts	TON	TOF (s⁻¹)
Fe ₉ S ₁₀ /Fe-MOF/NF-2	122.4	0.034
Fe-MOF/NF	3.6	0.0011
Fe ₉ S ₁₀ /NF	25.2	0.0072

Reference

1. F. Wu, X. X. Guo, Q. H. Wang, S. W. Lu, J. L. Wang, Y. B. Hu, G. Z. Hao, Q. L. Li, M. Q. Yang and W. Jiang, *J. Mater. Chem. A*, 2020, **8**, 14574-14582.
2. Q. L. Li, X. Li, K. Zhang, J. Q. He, Y. B. Lou and J. X. Chen, *Inorg. Chem. Commun.*, 2023, **153**, 110835.
3. Q. L. Li, K. Zhang, X. Li, J. Q. He, Y. B. Lou and J. X. Chen, *J. Alloys Compd.*, 2022, **920**, 165941.
4. S. S. Zheng, X. T. Guo, H. G. Xue, K. M. Pan, C. S. Liu and H. Pang, *Chem Commun (Camb)*, 2019, **55**, 10904-10907.
5. K. Wan, J. S. Luo, C. Zhou, T. Zhang, J. Arbiol, X. H. Lu, B. W. Mao, X. Zhang and J. Fransaer, *Adv. Funct. Mater.*, 2019, **29**, 1900315.
6. Y. Zhang, X. P. Shen, C. S. Song, Z. Y. Ji and F. H. Du, *J. Mater. Chem. A*, 2023, **11**, 8904-8911.
7. W. X. Lv, L. Zhu, L. Z. Cheng, Z. Wang, R. Zhang and W. Wang, *J. Appl. Electrochem.*, 2022, **52**, 1481-1489.
8. W. J. Song, M. Z. Xu, X. Teng, Y. Niu, S. Q. Gong, X. Liu, X. M. He and Z. F. Chen, *Nanoscale*, 2021, **13**, 1680-1688.
9. Y. J. Li, W. Y. Wang, B. J. Huang, Z. F. Mao, R. Wang, B. B. He, Y. S. Gong and H. W. Wang, *J.*

Energy Chem., 2021, **57**, 99-108.

10. D. X. Yang, Z. Su, Y. F. Chen, K. Srinivas, X. J. Zhang, W. L. Zhang and H. P. Lin, *Chem. Eng. J.*, 2022, **430**, 133046.
11. J. Liu, S. T. Wei, N. B. Li, L. Zhang and X. Q. Cui, *Electrochim. Acta*, 2019, **299**, 575-581.
12. C. Gan, Q. Jiang, X. Wu and J. Tang, *Mater. Today Chem.*, 2023, **27**, 101330.
13. Z. L. Chen, M. Liu and R. B. Wu, *J. Catal.*, 2018, **361**, 322-330.
14. X. Li, Z. K. Kou, S. B. Xi, W. J. Zang, T. Yang, L. Zhang and J. Wang, *Nano Energy*, 2020, **78**, 105230.